

## Acoustic superfocusing by solid phononic crystals

Xiaoming Zhou, M. Badreddine Assouar, and Mourad Oudich

Citation: [Applied Physics Letters](#) **105**, 233506 (2014); doi: 10.1063/1.4904262

View online: <http://dx.doi.org/10.1063/1.4904262>

View Table of Contents: <http://scitation.aip.org/content/aip/journal/apl/105/23?ver=pdfcov>

Published by the [AIP Publishing](#)

---

Over **600** Multiphysics  
Simulation Projects

[VIEW NOW >>](#)

COMSOL

The advertisement features a 3D simulation of a mechanical part with a colorful stress or temperature distribution. The text 'Over 600 Multiphysics Simulation Projects' is prominently displayed in white and blue. A blue button with white text says 'VIEW NOW >>'. The COMSOL logo is in the bottom right corner.

## Acoustic superfocusing by solid phononic crystals

Xiaoming Zhou,<sup>1,2,3</sup> M. Badreddine Assouar,<sup>1,2,a)</sup> and Mourad Oudich<sup>1,2</sup>

<sup>1</sup>CNRS, Institut Jean Lamour, Vandoeuvre-lès-Nancy F-54506, France

<sup>2</sup>Institut Jean Lamour, University of Lorraine, Boulevard des Aiguillettes, BP 70239, Vandoeuvre-lès-Nancy 54506, France

<sup>3</sup>Key Laboratory of Dynamics and Control of Flight Vehicle, Ministry of Education and School of Aerospace Engineering, Beijing Institute of Technology, Beijing 100081, China

(Received 8 October 2014; accepted 2 December 2014; published online 11 December 2014)

We propose a solid phononic crystal lens capable of acoustic superfocusing beyond the diffraction limit. The unit cell of the crystal is formed by four rigid cylinders in a hosting material with a cavity arranged in the center. Theoretical studies reveal that the solid lens produces both negative refraction to focus propagating waves and surface states to amplify evanescent waves. Numerical analyses of the superfocusing effect of the considered solid phononic lens are presented with a separated source excitation to the lens. In this case, acoustic superfocusing beyond the diffraction limit is evidenced. Compared to the fluid phononic lenses, the solid lens is more suitable for ultrasonic imaging applications. © 2014 AIP Publishing LLC.

[<http://dx.doi.org/10.1063/1.4904262>]

Acoustic superfocusing by metamaterials and phononic crystals has been a subject of much research in the past decade. The concept of superfocusing can be traced back to the Pendry's perfect lens,<sup>1</sup> and the lens system requires the ability of both the convergence of propagating waves and the participation of nonpropagative evanescent waves in the wave-focusing spot. The metamaterial superlens consists in a flat slab of composite medium with doubly negative mass density and bulk modulus. Mediums with these parameters exhibit negative refraction for incident waves and can also support surface resonant states to enhance the evanescent wave amplitudes.<sup>2</sup> Theoretical researches have been fully conducted to analyze the formation of surface states concerning both the fluid and solid nature of homogeneous metamaterials.<sup>2,3</sup> The structure design of the metamaterial superlens relies on accurate effective medium models, especially for prediction of evanescent wave behavior. Now it is still a hard task to find an optimum microstructure with good focusing performance.<sup>4-6</sup> Acoustic superfocusing can also be obtained in the phononic crystal lens consisting of a periodic array of inclusions in a fluid matrix.<sup>7</sup> Bragg scattering offers the opportunity for negative dispersion and wave convergence. There are two mechanisms for the phononic crystal lens to achieve the subwavelength focusing. One is based on the bound modes of the phononic crystal,<sup>8-10</sup> much like Lamb modes in a solid plate, which can be excited by evanescent waves emitted by the source. The lens with this ability is a fluid phononic crystal consisting of a triangular lattice of steel cylinders in methanol and surrounded by water, and superfocusing has been demonstrated both experimentally and theoretically. The other is by introducing a modulation on the surface of the phononic crystal;<sup>11</sup> this surface modulation is used to produce the surface states to amplify evanescent waves.

In this work, we focus on the solid phononic crystal lens with acoustic superfocusing in a water environment. The solid lens is studied considering the fact that they are more suitable for the human tissue environment. Compared with the only longitudinal mode in fluid, the modes in solid phononic crystals are more complex due to the coupling of longitudinal and transverse waves. While low-frequency modes are dominated by shear and rotational ones, negative dispersion of longitudinal waves usually appears at higher frequencies. This has been evidenced experimentally in a solid phononic crystal made of a triangular lattice of steel rods embedded in epoxy.<sup>12</sup> The other kind of solid crystal with a hollow metallic foam-like structure can also exhibit the negative dispersion behavior.<sup>13</sup> Focusing of elastic waves in a solid background has been realized by a solid crystal made of a square array of circular air holes perforated in a Duraluminium thin plate,<sup>14</sup> or by a gradient-index structure based on cylindrical stubs bonded on an aluminum plate.<sup>15</sup> These solid lenses are able to focus the propagating waves, however, lack in the ability of amplifying evanescent waves to overcome the diffraction limit. Inspired by the model proposed by Lai *et al.*,<sup>16</sup> who utilize four particles in a unit cell to create a locally resonant effect for longitudinal wave modes, we surprisingly find that the negative dispersion of longitudinal modes and surface states can be both produced in a simple crystal with four cylinders embedded in a solid hosting material. It is further found that the surface states can indeed provide the ability of coupling and amplifying the evanescent waves. This letter will report the properties of the band structure and surface states of this solid phononic crystal and demonstrates numerically acoustic superfocusing in the water environment.

The unit cell of the considered two-dimensional phononic crystal is shown in Fig. 1. The model is composed of four brass cylinders embedded in an Al-SiC foam matrix, and a vacuum cavity is arranged in the center. The lattice constant of the square lattice is 5 mm; the cylinder has a radius of 0.5 mm and is located at a distance of 1 mm from the

<sup>a)</sup>Author to whom correspondence should be addressed. Electronic mail: Badreddine.Assouar@univ-lorraine.fr

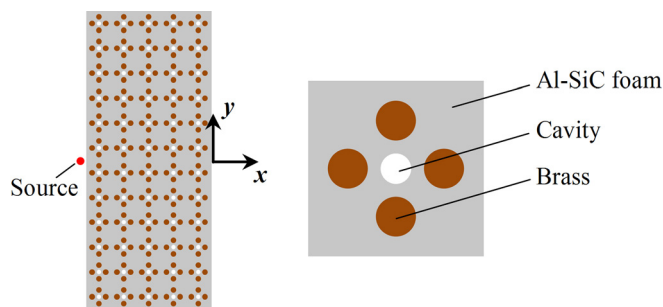


FIG. 1. The model of the studied superlens whose unit cell is composed of four brass cylinders embedded in an Al-SiC foam matrix with a vacuum cavity arranged in the center.

center; the radius of the cavity is 0.4 mm. The Young’s modulus, Poisson’s ratio, and mass density are, respectively, 70 MPa, 0.3, and 72 kg/m<sup>3</sup> for the foam, and 104 GPa, 0.37, and 8500 kg/m<sup>3</sup> for the brass. Based on the finite element simulation, we calculate the band structure of the infinitely periodic crystal in the principal symmetry directions of the Brillouin zone, as shown in Fig. 2(a). The first two branches starting from the  $\Gamma$  point correspond to quasi-transverse and quasi-longitudinal modes. The next three branches are attributed to the rotation and shear deformation modes, while the sixth branch with a negative slope in both  $\Gamma X$  and  $\Gamma M$  directions corresponds to the longitudinal mode, which is of interest in this work. The displacement amplitude distribution of the eigenstate at the  $\Gamma$  point in this branch (marked with “A”) is plotted in Fig. 2(b), where the arrows indicate the direction of motion. The eigenstate is clearly a monopolar response as evidenced by the collective motion of four

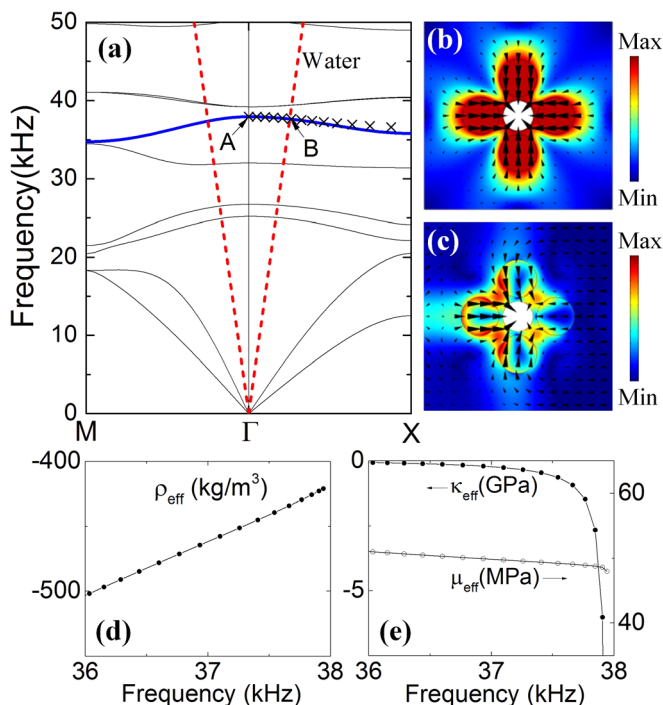


FIG. 2. (a) The band structure of a square lattice of the infinite crystal (solid line), the dispersion curve of the water (dashed line), and the dispersion curve given by effective medium prediction (cross); (b) and (c) the displacement distributions of the unit cell corresponding to the eigenstates marked in (a) with “A” and “B,” respectively; the retrieved effective mass density  $\rho_{\text{eff}}$  (d) and effective bulk and shear moduli  $\kappa_{\text{eff}}$  and  $\mu_{\text{eff}}$  (e).

cylinders toward or outward from the center. Notice that the arranged cavity is for the purpose of easy bulk deformation near the center region. Since acoustic focusing in water is concerned, we illustrate the straight dispersion curve of water in Fig. 2(a). This dispersion curve intercepts the longitudinal wave branch with the negative curvature at frequencies of 37.65 Hz and 37.4 Hz in the  $\Gamma X$  and  $\Gamma M$  directions, respectively. We have verified that the equifrequency contour is nearly circular at these frequencies (see Fig. 3). The result means the all angle negative refraction of the phononic crystal with an effective index  $-1$  relative to water, which is the key property required for the convergence of propagating waves.

We further show in Fig. 2(c) the eigenstate of the phononic crystal in the intersection point labeled with “B.” It is seen that away from the  $\Gamma$  point, the pure monopolar state turns into a state of the combination of the monopolar and dipolar ones. In this state, cylinders move toward the center uniformly, but with a little different displacement amplitudes; this provides the dipolar response. From the eigenstate analyses, one readily finds that the wave behavior of the studied sonic crystal is dominated by the relative motions of local cylinders, while not by the interference among cells, as evidenced by the weak field strength near the edge of the cell. The phenomenon is very similar to that observed in the hybrid elastic solids,<sup>16</sup> which have been recognized as metamaterials with doubly negative mass density and bulk modulus. In our model, the wavelength in the foam corresponding to the  $\Gamma$  point frequency is 6 times bigger than the lattice constant; we are not convinced that this value falls within the effective medium description of metamaterials. However, if the effective medium model is forced to apply for the structure, effective parameters can be achievable according to surface integration method.<sup>16</sup> The predicted branch in the  $\Gamma X$  direction is plotted by the cross in Fig. 2(a) and shows the agreement with the band structure results. Both of the retrieved effective mass density  $\rho_{\text{eff}}$  and bulk modulus  $\kappa_{\text{eff}}$  are found to be negative, as shown in Figs. 2(d) and 2(e). Though not based on a reliable assumption, the effective medium analysis may explain the formation of negative curvature of the longitudinal wave branch and more

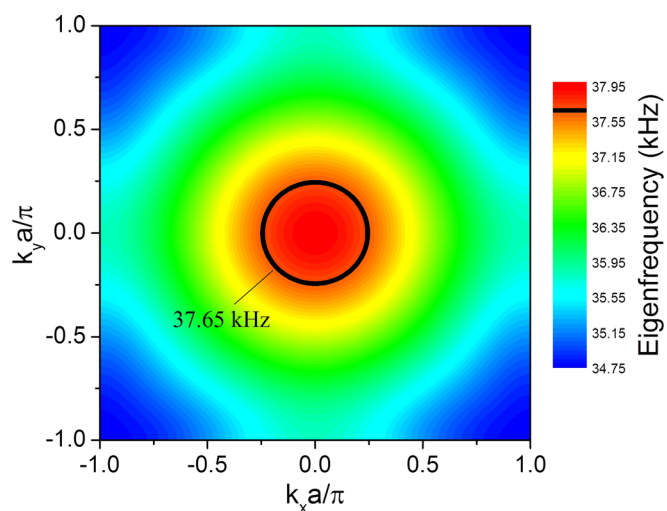


FIG. 3. The eigenfrequency contour plot of the solid phononic crystal.

importantly imply the presence of the surface states associated to the double negativity.

To examine the property of the surface states of the studied solid crystal, the supercell model consisting of  $N$  cells in water as shown in Fig. 4(a) is used for calculating the band structure in the direction parallel to the water-lens interface. The periodic boundary conditions are imposed on the top and bottom boundaries of the supercell. Mass density and sound velocity of water are set as  $1000 \text{ kg/m}^3$  and  $1490 \text{ m/s}$ . Figures 4(b) and 4(c) show, respectively, the band structure results of the supercell comprising  $N=8$  and  $N=10$  unit cells of the phonic structure. The dispersion curves of water (the red dashed line) and longitudinal wave branch (the blue solid line) of the phonic crystal are also included for comparison. For the modes on the right of the water line, acoustic fields in water are evanescent, while in solid crystals, we have propagative modes which fall below the longitudinal wave branch. These propagating modes have the same physics with Lamb modes in pure plate and are dependent on the finite thickness, namely, the number of unit cells. The modes that fall above the longitudinal wave branch and in the right of the water line are surface modes bound to the water-lens interface. Shown in Fig. 4(d) are the eigenstates of the surface mode at frequency of  $37.65 \text{ kHz}$  for the case of  $N=8$ , and it is indeed observed that the wave fields are strongly confined near to the interface. Moreover, these surface modes are almost irrelevant to the crystal thickness, meaning the weak coupling between two interfaces of the lens.

In order to produce the super-resolution focusing, evanescent waves emitted from a point source must excite and couple the surface mode of the phonic crystal. This

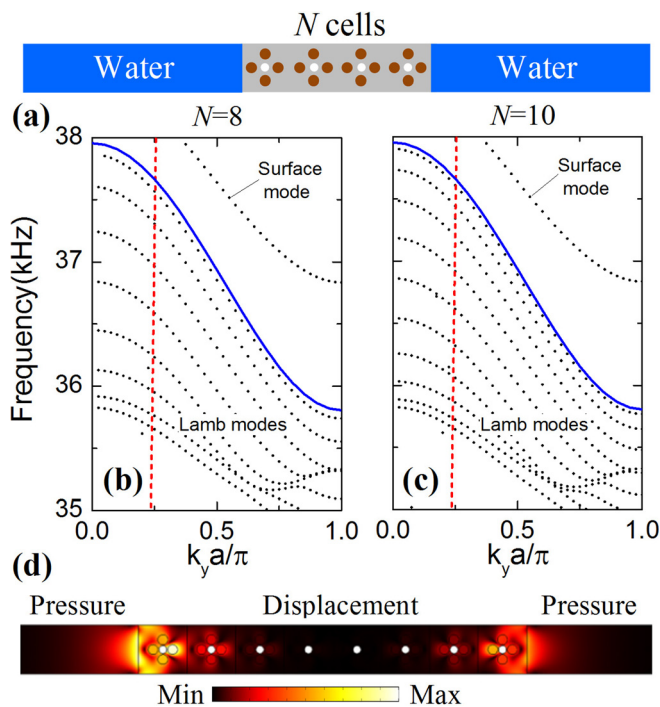


FIG. 4. (a) The supercell model for calculation of acoustic bulk (Lamb) and surface modes of a  $N$ -layers phonic crystal. Dispersion curves (solid circle) of acoustic bulk and surface modes of phonic crystals composed of (b)  $N=8$  and (c)  $N=10$  layers. (d) The field distribution of the eigenstate of acoustic surface mode of the eight-layer crystal at frequency  $37.65 \text{ kHz}$ .

normally happens if the source lies in the near field of the crystal. Moreover, the coupling should be efficient when the point source is placed between the unit cells, because the pressure amplitude reaches the maximum in front of each cell, as observed in Fig. 4(d). Thus, the maximum displacement amplitude is achieved between the unit cells in both the fluid and solid regions. Acoustic focusing by the solid phonic crystal is studied based on the commercial software, COMSOL Multiphysics. The lens under study comprises 8 cells in thickness and 60 cells in width. This means that the thickness  $d$  of the lens is about one wavelength ( $\lambda$ ) in water corresponding to the operating frequency  $37.65 \text{ kHz}$ , and the aspect ratio of the lens is 7.5, which suffices to avoid the imaging distortions.<sup>8</sup> Figure 5(a) shows the contour plot of the normalized pressure fields, in which a point source is placed at a distance of  $s=2 \text{ mm}$  ( $\lambda/20$ ) from the surface of the slab lens. It can be seen that a focusing spot appears on the right side of the crystal. According to acoustic ray tracing, the distance  $i$  of the focusing spot should perfectly match  $i=d-s$ . Since  $s \ll d$ , the focusing distance is approximately equal to the lens thickness, i.e.,  $i \approx d$ . We therefore examine the lateral distribution of pressure intensity in the image line located at  $x=d$ , as illustrated in Fig. 5(b). The result clearly demonstrates the sub-diffraction-limited acoustic focusing with a spatial resolution of  $0.41\lambda$ , which is defined as the full width at half maximum (FWHM) of the transmission peak measured at the basis of the peak.<sup>9</sup> The presence of the superfocusing emphasizes the role of the crystal's surface modes in amplification of evanescent

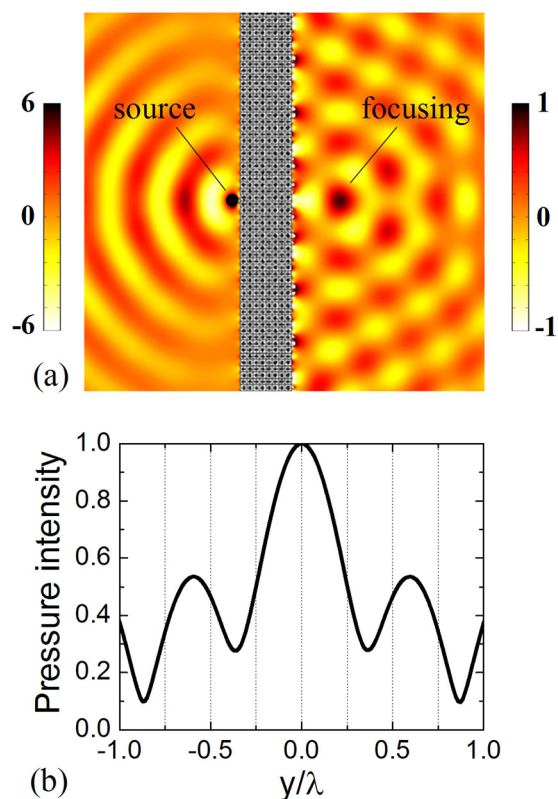


FIG. 5. (a) Pressure field distribution of a point source with an oscillating frequency  $37.65 \text{ kHz}$  placed at a distance of  $2 \text{ mm}$  from the surface of an eight-layer phonic crystal. (b) Lateral distribution of pressure intensity across the focusing spot ( $i=40 \text{ mm}$ ) behind the lens.

waves. It is noted that the proposed crystal structure has not been optimized for the purpose of the matched impedance to the background; as a result, the pressure levels are different in the source and image regions, as indicated by different color scales in Fig. 5(a). Further optimization studies are being conducted regarding this aspect.

In this work, we have proposed a solid phononic crystal lens capable of acoustic superfocusing beyond the diffraction limit. We have found a mechanism by which evanescent waves can be amplified in a solid phononic crystal composed of four rigid cylinders embedded in a solid matrix. From the band structure analyses, the negative curvature of the longitudinal wave branch can be attributed to relative motions of cylinders and associated very well to the double negativity. This may imply the existence of the surface mode that accounts for the evanescent wave amplification. Acoustic superfocusing by the solid lens is finally assessed by numerical simulations. The proposed superlens is simple in geometry and based on physically realizable materials. In addition, the wavelength of the focused wave is much larger than the lattice constant of the solid crystal, and the relevance between the sensitivity of the wave focusing to the crystal array imperfections should be very low. This will facilitate the experimental realization of the lens. The solid nature of the proposed lens makes it more suitably used for ultrasonic medical imaging in human tissue environment.

M.B.A. and M.O. would like to thank “La Région Lorraine” and the “FEDER” for its financial supports. X.Z.

acknowledges supports from the National Natural Science Foundation of China (Grant No. 11172038) and Program for New Century Excellent Talents in University (Grant No. NCET-11-0794).

- <sup>1</sup>J. B. Pendry, *Phys. Rev. Lett.* **85**(18), 3966–3969 (2000).
- <sup>2</sup>K. Deng, Y. Ding, Z. He, H. Zhao, J. Shi, and Z. Liu, *J. Appl. Phys.* **105**(12), 124909 (2009).
- <sup>3</sup>M. Ambati, N. Fang, C. Sun, and X. Zhang, *Phys. Rev. B* **75**(19), 195447 (2007).
- <sup>4</sup>S. Zhang, L. Yin, and N. Fang, *Phys. Rev. Lett.* **102**(19), 194301 (2009).
- <sup>5</sup>G. Sébastien, M. Alexander, P. Gunnar, and S. A. Ramakrishna, *New J. Phys.* **9**(11), 399 (2007).
- <sup>6</sup>X. N. Liu, G. K. Hu, G. L. Huang, and C. T. Sun, *Appl. Phys. Lett.* **98**(25), 251907 (2011).
- <sup>7</sup>X. Zhang and Z. Liu, *Appl. Phys. Lett.* **85**(2), 341–343 (2004).
- <sup>8</sup>J. F. Robillard, J. Bucay, P. A. Deymier, A. Shelke, K. Muralidharan, B. Merheb, J. O. Vasseur, A. Sukhovich, and J. H. Page, *Phys. Rev. B* **83**(22), 224301 (2011).
- <sup>9</sup>A. Sukhovich, L. Jing, and J. H. Page, *Phys. Rev. B* **77**(1), 014301 (2008).
- <sup>10</sup>A. Sukhovich, B. Merheb, K. Muralidharan, J. O. Vasseur, Y. Pennec, P. A. Deymier, and J. H. Page, *Phys. Rev. Lett.* **102**(15), 154301 (2009).
- <sup>11</sup>Z. He, X. Li, J. Mei, and Z. Liu, *J. Appl. Phys.* **106**(2), 026105 (2009).
- <sup>12</sup>C. Croëne, E. D. Manga, B. Morvan, A. Tinel, B. Dubus, J. Vasseur, and A. C. Hladky-Hennion, *Phys. Rev. B* **83**(5), 054301 (2011).
- <sup>13</sup>A. C. Hladky-Hennion, J. O. Vasseur, G. Haw, C. Croëne, L. Haumesser, and A. N. Norris, *Appl. Phys. Lett.* **102**(14), 144103–144104 (2013).
- <sup>14</sup>M. Dubois, M. Farhat, E. Bossy, S. Enoch, S. Guenneau, and P. Sebbah, *Appl. Phys. Lett.* **103**(7), 071915 (2013).
- <sup>15</sup>X. Yan, R. Zhu, G. Huang, and F. G. Yuan, *Appl. Phys. Lett.* **103**(12), 121901 (2013).
- <sup>16</sup>Y. Lai, Y. Wu, P. Sheng, and Z. Q. Zhang, *Nat. Mater.* **10**(8), 620–624 (2011).